Article

Multi-Analytical Investigation of the Oil Painting *"Il Venditore di Cerini"* by Antonio Mancini and Definition of the Best Green Cleaning Treatment

Andrea Macchia [1,2,*], Chiara Biribicchi [1], Paola Carnazza [3], Stefania Montorsi [4], Nausicaa Sangiorgi [5], Giuseppe Demasi [6], Fernanda Prestileo [7], Eleonora Cerafogli [4], Irene Angela Colasanti [4], Helene Aureli [4], Margherita Zappelli [4], Michela Ricca [2] and Mauro Francesco La Russa [2]

1. Department of Earth Sciences, University of Rome La Sapienza, P.le Aldo Moro 5, 00185 Rome, Italy; chiara.biribicchi@uniroma1.it
2. Department of Biology, Ecology and Earth Sciences (DiBEST), University of Calabria, Via Pietro Bucci, 87036 Arcavacata, Italy; michela.ricca@unical.it (M.R.); mlarussa@unical.it (M.F.L.R.)
3. Galleria Nazionale d'Arte Moderna e Contemporanea, Viale delle Belle Arti 131, 00197 Rome, Italy; paola.carnazza@beniculturali.it
4. YOCOCU, Youth in Conservation of Cultural Heritage, Via T. Tasso 108, 00185 Rome, Italy; montorsi.stefania@gmail.com (S.M.); cerafogli.1559339@studenti.uniroma1.it (E.C.); colasanti.1748988@studenti.uniroma1.it (I.A.C.); heleneaureli94@gmail.com (H.A.); zappelli.1692139@studenti.uniroma1.it (M.Z.)
5. Independent Researcher, Via del Broaldo 6, 40064 Ozzano, Italy; nausi.sangiorgi@hotmail.it
6. Independent Researcher, Via Arci 9, 02032 Fara In Sabina, Italy; giuseppedemasi11@yahoo.it
7. CNR-ISAC, Via Fosso del Cavaliere 100, 00133 Rome, Italy; fernanda.prestileo@cnr.it
* Correspondence: andrea.macchia@uniroma1.it

Abstract: This paper describes the multi-analytical approach implemented for the study of the oil painting *Il Venditore di Cerini* made by Antonio Mancini in 1878. The research was carried out to characterize both the original stratigraphy and the alleged non-original varnish on the surface. SEM/EDS analysis showed the presence of pigments already detected in other paintings by Antonio Mancini. Multispectral imaging, DinoLite microscope, and FT-IR ATR spectroscopy revealed significant data regarding the invention of the "graticola" method—a technique implemented by Mancini to respect the proportions of the figures—also proving the presence of an aged layer of non-original shellac on the surface. The yellow/brownish tone of the varnish was hiding the real shapes of the figure, requiring a selective removal of the aged coating. The proposed cleaning systems were chosen among the green chemical alternatives present in the market, aiming at promoting a sustainable development in the Cultural Heritage field. The selection was made according to the Fd parameter of the cleaning systems—which defines the energy from dispersion forces between molecules—in relation to what is defined in the literature as the suitable Fd value for the removal of the shellac. The best-performing green cleaning system proved to be the Polar Varnish Rescue GEL—a gelled acetals mixture developed by YOCOCU APS—for its effectiveness in selectively remove the aged shellac while preserving the integrity of the original stratigraphy.

Keywords: green; conservation; sustainability; cultural heritage; Antonio Mancini; shellac; FTIR ATR; SEM/EDS; acetals; cleaning; surfactant

1. Introduction

Admired by many of his contemporary painters for the engaging truth of his painting and portraits, Antonio Mancini (1852–1930) was one of the most original personalities of Italian realist painting [1]. He used a painting technique in which color had also a tridimensional shape, in an era where only a few painters were following a similar path [2,3].

Mancini showed notable stylistic evolution and remarkable technical peculiarities. He started using a method of his own invention for the execution of portraits in 1889 [4]. It is called the "graticola" method because the artist used to place a cotton thread gridiron in front of the posing figure and another one on the canvas, measuring the distances between the threads on the first and transferring them on the second frame, maintaining the same proportions (Figure 1a). Once the painting was completed and the frame was removed from the canvas, the typical and particular "Mancinian" imprint was generated on it, impressed by the threads that arise from the thick layer of color [3]. Although the eccentricity of Mancini's stylistic evolution is evident, his palette was already set in 1870s, with few exceptions, remaining so until the end of his career [2]. In the 1870s and 1880s, when Impressionist painters or others such as Giovanni Boldini abandoned the use of colors such as Chrome Yellow and Prussian Blue, Antonio Mancini maintained the same palette. Indeed, the materials used by the artist have been thoroughly investigated and technical information on the matter is already well known. Mancini used to paint mostly on canvas, while only few paintings were created exploiting panels as supports. Some of his works show an industrial ground layer made of Lead White and Zinc White, sometimes including calcium carbonate and barium sulphate, while another work shows a non-homogeneous ground layer applied by the artist and made of Lead White and barium sulphate. The pigments detected in most of his works are characteristic as well and can be identified as: Lead White, Zinc White, Chrome Orange, Prussian Blue, Cobalt Blue, Ultramarine Blue, Cerulean Blue, Cadmium Yellow, Chrome Yellow, Naples Yellow, Strontium Yellow, Red Lake, Carbon Black, Bone Black, Ochre, Green Earth, Cassel Earth, Iron Oxides, Chrome Oxide Green, Schweinfurt Green, Vermilion, and Cobalt Violet [2]. Eventually, the analyses made on his paintings always detected an oil binder [2].

(a)   **(b)**
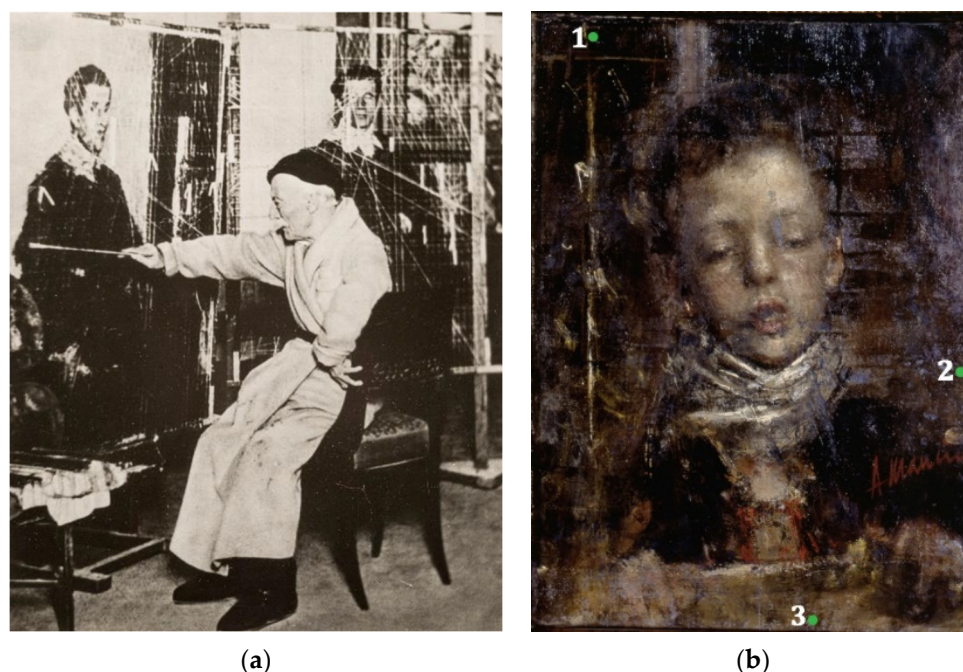
Figure 1. (**a**) Antonio Mancini while using the "graticola" method. Credits: Cinzia Virno; (**b**) Antonio Mancini, *Il Venditore di Cerini* (1878), Galleria Nazionale d'Arte Moderna e Contemporanea, Rome (IT): image before the intervention with the indication of the sampling areas.

As a confirmation of this, *Il Venditore di Cerini*—the oil painting on canvas made by Antonio Mancini in 1878 (Figure 1b)—shows the typical Mancini's technique and palette [2].

The wet-on-wet construction testifies to the rapid execution of the work, while the Caravaggesque structure of the painting brings the magnificently detailed figure standing out against the dark background, showing similarities with *Saltimbanco con Violino* made

in 1878. Therefore, the present work aims at integrating the already available information on Antonio Mancini's artistic technique through the analysis of the materials and the stratigraphy of *Il Venditore di Cerini*. In this case, the usual reasons that give meaning to analytical research—such as the study of materials and execution technique—are enriched by further needs, namely, the characterization of the finishing layer, which is supposed to be non-original, mainly due to the absence of a varnish in all of Mancini's paintings analyzed thus far [2].

The multi-analytical approach implemented enabled the acquisition of significant elements to characterize the stratigraphy and the constituent materials of the painting, also guiding the cleaning treatment performed on the artwork [5]. Non-invasive analyses were carried out in the Restoration Laboratories of the Galleria Nazionale d'Arte Moderna e Contemporanea in Rome, enabling the selection of the sampling areas and providing substantial data regarding the artistic technique and the presence of a non-original varnish. However, the non-invasive diagnostics implemented could not answer questions regarding the characterization of the stratigraphy and the composition of the constituent materials. Thus, micro-invasive analyses, namely, Fourier Transform Infrared Spectroscopy (FT-IR) in Attenuated Total Reflectance mode (ATR), and Scanning Electron Microscopy coupled with an Energy Dispersion microanalytical System (SEM/EDS), were carried out at the YOCOCU APS laboratory in Rome [6].

Then, cleaning tests were performed to define a suitable cleaning system to selectively remove the identified aged shellac varnish which hid the original features of the figure. The cleaning was supposed to comply with the principles of Green Chemistry [7–9] and minimum intervention, to have a suitable degree of solubilization of the varnish, aiming at obtaining the maximum performance while operating in the least invasive way possible. The system also needed to be easy to apply, allowing for the gradual removal of the aged material. Hence, we considered some green alternatives already available in the market as more eco-friendly solutions to replace hazardous substances that are still widely used in the conservation field, aiming at promoting sustainable development [10].

The scientific literature and the Teas' triangle identify ethanol as a suitable solvent for unaged shellac [11–13]. However, recent research explored the potentialities of both pure PVA–borax gel and PVA–borax gel loaded with acetone to clean a highly oxidized shellac layer from a 15th-century egg tempera wood panel [14,15]. Indeed, over the years, new perspectives have been opened by the application of materials science, colloid science, and interface science frameworks to conservation, generating a breakthrough in the development of greener functional materials for the cleaning of cultural heritage, such as acrylamide gels, PHB-based gels, PVA-based gels, MMA-based organogels, and semi-interpenetrating polymer networks of p(HEMA)/PVP [16–19]. Furthermore, the effects of neodymium (Nd):YAG, holmium (Ho):YAG, and erbium (Er):YAG laser sources, in different operative modes, were specifically tested for the removal of shellac layers from wall painting mock-ups [20]. We chose to exploit the potentialities of new green materials developed by the YOCOCU APS team and recently presented at the IV edition of the Green Conservation of Cultural Heritage Conference [21]. Specifically, the Green Varnish Rescue and the Polar Varnish Rescue in the gelled forms—using hydroxypropylcellulose (Klucel® G) at the concentration of 5% *w/v*—were tested as sustainable alternatives to more common solvents [10,22,23]. The selection was made based on the inner low toxicity of the constituent solvents with respect to other methodologies. Indeed, the Green Varnish Rescue is composed of a mixture of acetals, while the Polar Varnish Rescue is made of a mixture of acetals coupled with an anionic surfactant, which are known to be non-toxic chemicals [24]. Indeed, while the sustainability of cleaning methods is often pursued through the development of delivery systems capable of a gradual release of the substance, the "greenness" of these new products relies on their high boiling points and the absence of hazard symbols [22,23]. Moreover, the proposed products can be easily applied on the artwork's surface, thus providing a wide-ranging solution available for restorers. In this paper, we propose hydroxypropylcellulose (Klucel® G) as a thickening agent for both the

Green Varnish Rescue and the Polar Varnish Rescue to provide a first demonstration of their use in the gelled form. However, the implementation of other delivery systems could be considered in future experiments to evaluate their applicability.

2. Materials and Methods

Multispectral imaging was carried out using visible, ultraviolet (UV), and infrared (IR) spectrum bands. UV fluorescence was used to identify and characterize the presence of film-forming substances on the surface, while Mid- and Near-Infrared spectrum bands allowed verification of the presence of IR-active materials. The investigation was carried out with the Madatec multispectral system consisting of a Samsung NX500 28.2 MP BSI CMOS camera, and Madatec spotlights, using the following wavelengths: 365 nm (UV), 440 nm (blue), and 532 nm (green). Observations of induced fluorescence were obtained using the following filters: HOYA UV-IR filter cut 52 and Yellow 495 52 mm F-PRO MRC 022; three different IR filters at 850 nm were used for IR reflectography.

The examination of the surface morphology was carried out using the portable optical microscope DinoLite AM411-FVW. It was performed using different magnifications, from $40\times$ to $220\times$, and three illumination modes: visible light (VIS), ultraviolet light (UV), and ranking light (VIS-RAD). Both the examination of the surface with DinoLite and multispectral imaging enabled the selection of the more significative sampling areas. Three samples were taken from the upper, right, and bottom border of the painting to make the sampling as minimally invasive as possible (Figure 1b). Sample 1 includes the ground layer, the primer, and the paint layers without the varnish; sample 2 consists of the original canvas, the ground layer, the primer, the paint layers, and the varnish, while sample 3 includes the ground layer, the primer, the paint layers, and the varnish.

FTIR spectroscopy was performed on samples 2 and 3 without pretreatment. Spectra were collected on sample 2 by placing both the front and the back of the sample on the diamond of the ATR. The front consists of the layer on the top, while the back consists of the original canvas. The samples were studied by Fourier Transform Infrared spectroscopy (FT-IR) in ATR mode to characterize the painting's materials in the stratigraphy at the functional-group level. The IR spectra were collected using the Nicolet Summit FTIR spectrometer equipped with the Everest™ Diamond ATR accessory, which allows analysis in attenuated total reflectance (ATR). This technique allows direct examination of solid and liquid samples without using preparation techniques with an instrumental resolution of 8 cm^{-1}. A total of 32 scans were performed on each sample, and the respective spectra were analyzed using the database edited by Vahur [25,26], using the database library and the scientific literature.

SEM/EDS analyses were performed on samples 1 and 2 to characterize the painting's materials in the stratigraphy at the elemental level using a Tescan microscope with INCA 2000 EDS. SEM/EDS allows the analysis of samples without any pre-treatment, being able to operate even in non-high-vacuum conditions or in high vacuum with very low beam intensity. For the present study, we chose the low-vacuum mode (15 Pa) with a 30 kV voltage of electron acceleration without any pretreatment of the sample and using the detector for backscattered electrons. SEM–EDS analysis was performed in both variable and high-vacuum modes, allowing the determination of the elements based on boron. Three samples were previously observed at the Optical Microscope and then analyzed to determine their stratigraphy and the composition of the various layers.

The cleaning systems listed in Table 1 were tested as potential solutions for the selective removal of the aged varnish which was on the painting's surface. The choice of operating with them was made after the identification of the suitable Fd parameter—i.e., the energy from dispersion forces between molecules—achieved through the implementation of the solubility test developed by P. Cremonesi [27–29]. It was carried out using the following products: Ligroine with a boiling point of 100–140 °C (Carlo Erba Reagents s.r.l., CAS n. 8032-32-4) and Ethanol Absolute Anhydrous (Carlo Erba Reagents s.r.l., CAS n. 64-17-5). During the execution of Paolo Cremonesi's test, the best-performing solution turned out to

be the mixture of Ligroine and Ethanol Absolute Anhydrous in relative amounts of 70% and 30%, respectively. Then, the proposed cleaning systems were chosen among the green chemical alternatives already present in the market, leaving aside other green solutions such as biotechnology. Hydroxypropylcellulose (Klucel® G, CTS® s.r.l., CAS n. 64742-49-0) was used as a gelling agent for the Green Varnish Rescue GEL and the Polar Varnish Rescue GEL [22,23]. Klucel G® was directly added to the products at room temperature, then magnetic stirring was used to provide a homogeneous gel.

Table 1. Tested cleaning systems.

ID	Solvent	Manufacturer	Composition	Application Method
1	Ethanol Anhydrous Absolute	Alfa Aesar	Absolute	Swab
2	Green Varnish Rescue	YOCOCU APS	Acetals' mixture	Swab
3	Green Varnish Rescue GEL	YOCOCU APS	Acetals' mixture in hydroxypropylcellulose (5% w/v)	GEL application for 120 s using Japanese paper
4	Nanorestore Cleaning®	Center for Colloid and Surface Science—CSGI	Nanostructured water-based fluid with anionic surfactant and mixture of 1-pentanol, ethyl acetate, and propylene carbonate	Swab
5	Polar Varnish Rescue GEL	YOCOCU APS	Anionic surfactant and acetal in hydroxypropylcellulose (5% w/v)	GEL application for 120 s using Japanese paper
6	Deionized water	-	Pure	Swab

Cleaning systems n° 1, 2, 4, and 6 were simply applied using a swab and little mechanical action to evaluate the removal of the aged varnish (Table 1) [30]. Cleaning systems n° 3 and 5 were applied using two sheets of Japanese paper as an intermediate layer to avoid the release of hydroxypropylcellulose's residues on the surface. Then, Japanese paper was removed, and a dry swab was used to clean the surface from the extra solvent (Table 1).

3. Results

3.1. Multi-Analytical Process

3.1.1. DinoLite Portable Optical Microscope

Portable optical microscopy analysis examined the artwork's surface, assessing the presence of many color gaps which allowed observation of a blue layer underneath, namely, a pigmented primer (see Section 3.1.4). The surface appears to be covered by an orange/brown varnish that shows yellow fluorescence under UV light (Figure 2a,c). Furthermore, large brushstrokes alternate with thin layers of color that use the clear and translucent primer to produce light effects (Figure 3a,c). Eventually, fibers embedded in the paint layer were detected (Figure 4a). They could be ascribed to the "graticola" technique [4] or added voluntarily by the artist, in the same way Mancini did in other paintings [2], or even related to previous restoration treatments, as attested by the re-lining of the artwork.
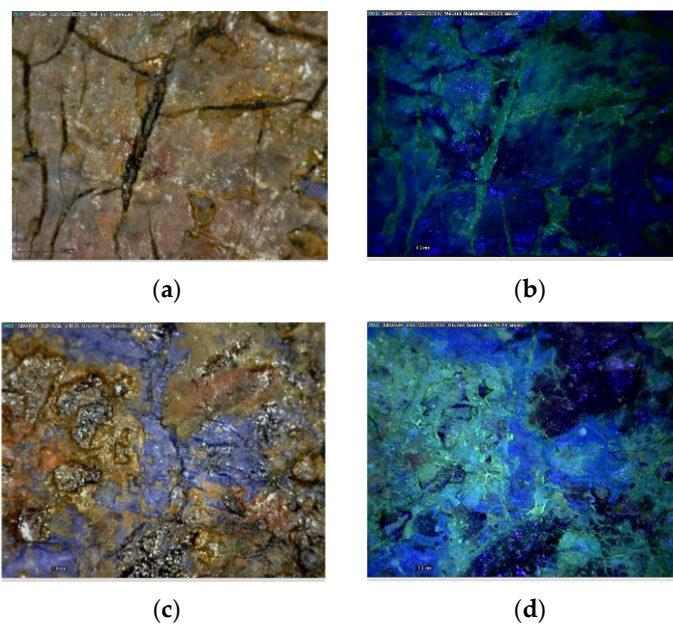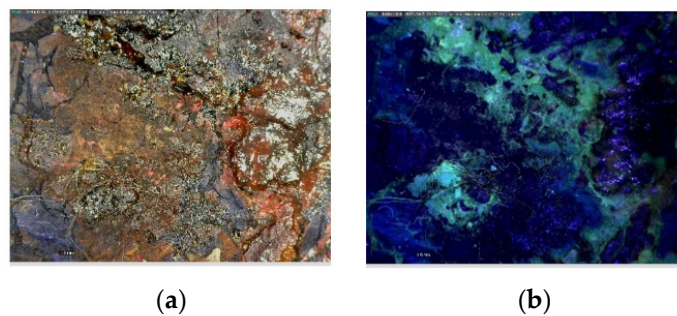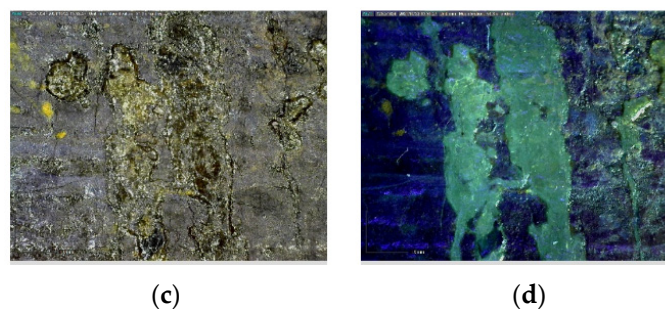
Figure 2. DinoLite images of the painting's surface (50×) in VIS light (**a**,**c**) and UV light (**b**,**d**); brownish varnish (**a**,**b**) and both the varnish and the paint layer (**c**,**d**).
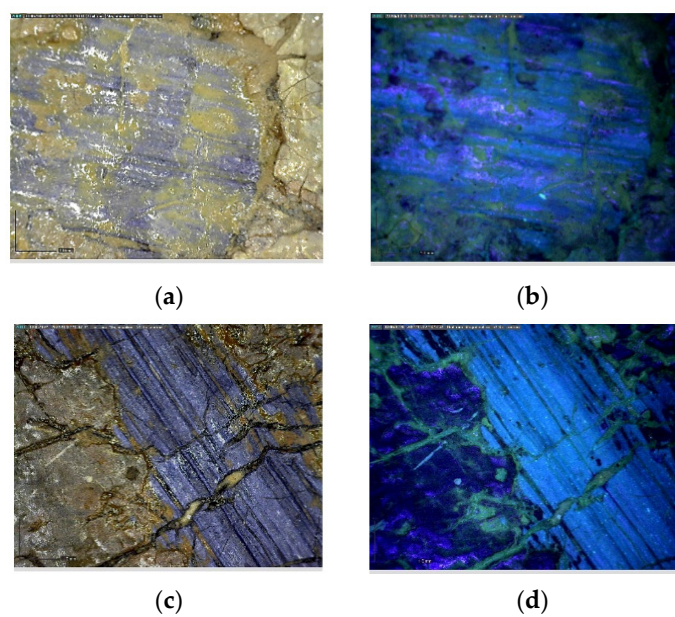
Figure 3. DinoLite images of the painting's surface (50×) in VIS light (**a**,**c**) and UV light (**b**,**d**); primer layer and color gap (**a**,**b**) and both primer and paint layers (**c**,**d**).

Figure 4. *Cont.*

(c)   (d)

Figure 4. DinoLite images of the painting's surface (50×) in VIS light (**a**,**c**) and UV light (**b**,**d**); retouched areas and fibers embedded in the paint layers (**a**–**d**).

3.1.2. Multispectral Imaging

Multispectral imaging allowed a deeper understanding of the painting's artistic technique and state of conservation. The images acquired in visible illumination mode highlight the presence of the so-called "Mancinian" imprint (Figure 5). It is peculiar that it can be seen on *Il Venditore di Cerini*, a painting made in 1878, namely, eleven years before the date declared in previous research [4].
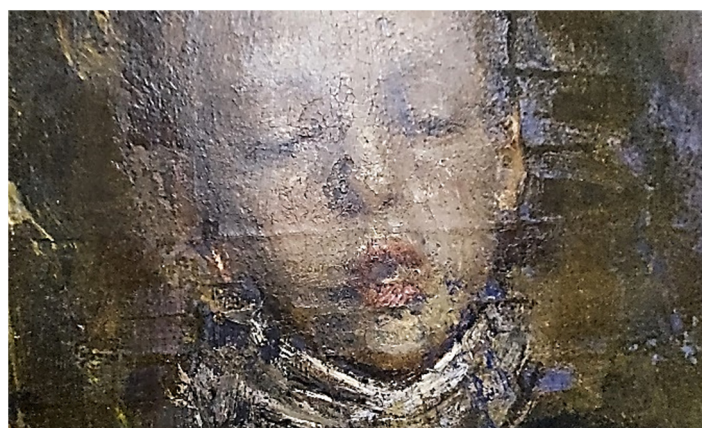

**Figure 5.** Detail of the area where the "Mancinian" imprint is visible.

The fluorescence induced by UV radiation showed that the varnish is non-homogeneously spread over the entire surface, being thicker on the left part of the figure, when seen from the front (Figure 6a–f). Additionally, in the picture acquired in UV-induced fluorescence, the signature of the artist disappears completely, proving that it has been applied on top of Mancini's signature (Figure 6c,f). Consequently, the varnish cannot be traced back to the execution stage. Moreover, none of the works by Mancini analyzed thus far shows a varnish in their stratigraphy, proving that the artist did not used to cover his paintings with a finishing layer.

Infrared reflectography unearthed the original definition of the figure shape, which could be seen more clearly since it was partially covered by the non-original aged varnish (Figures 7a and 8a–c). The forms appear to be only slightly outlined, without showing a preparatory drawing underneath, which means absence of a predefined graphic setting. Indeed, no second thoughts or modifications during the work can be detected in the reflectograms, as in other works of the artist, proving the rapid execution of Mancini's paintings. The transparency of the varnish under IR radiation uncovered the widespread craquelure of the paint layers, while the low contrast between the paint film and the color gaps proved that the former consists of a very thin layer. Furthermore, it was possible to see the previously retouched areas which differ from the original layers under IR radiation, being darker.
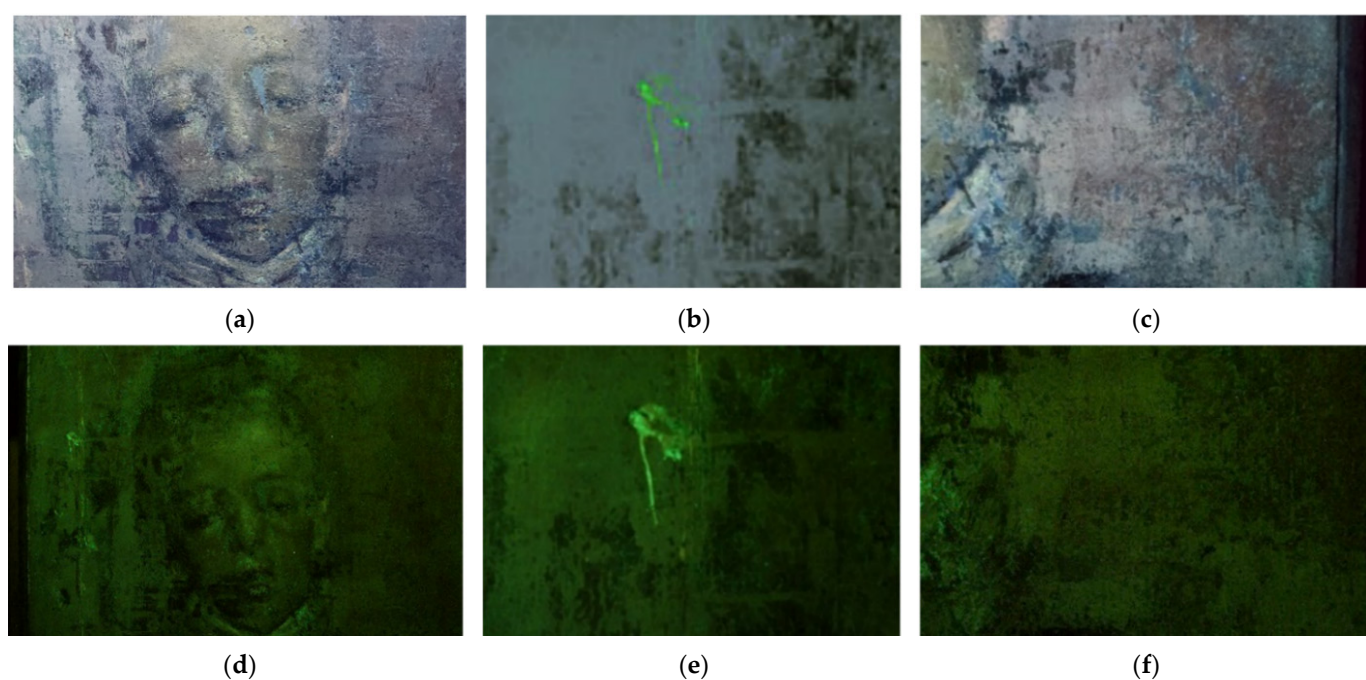
Figure 6. Multispectral imaging. Fluorescence induced by UV radiation: detail of the face (**a**), detail of the left side of the painting (**b**), and detail of the signature (**c**). Fluorescence induced by UV light using the HOYA UV-IR filter cut 52 and Yellow 495 52 mm F-PRO MRC 022: detail of the face (**d**), detail of the left side of the painting (**e**), and detail of the signature (**f**).
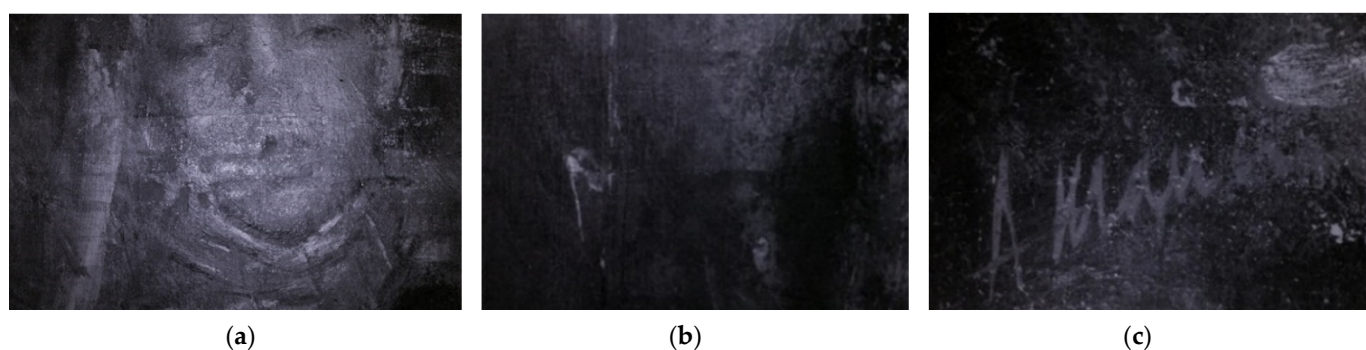
Figure 7. Multispectral imaging. Infrared reflectography using IR filters at 850 nm: detail of the face (**a**), detail of the left side of the painting (**b**), and detail of the signature (**c**).
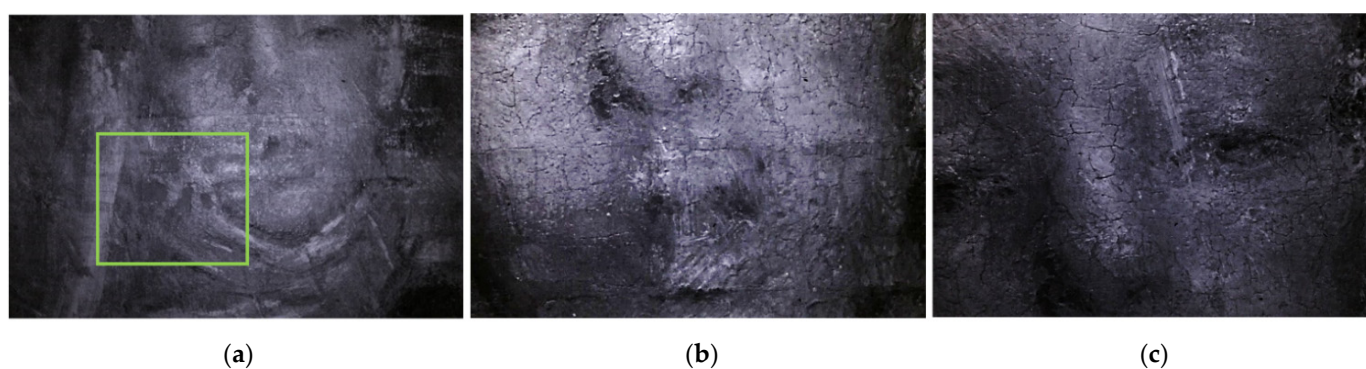
Figure 8. Multispectral imaging. Infrared reflectography using IR filters at 850 nm: detail of the face and retouched areas circled in green (**a**), detail of the lips (**b**), and detail of the nose and the eyes (**c**).

Eventually, the face of the figure was subjected to an even more extensive investigation by IR reflectography to highlight eventual variations made by the artist during the creation of the work as well as possible restoration treatments (Figure 8a). It appears that the face has been built by superimposing thin paint layers on a likewise thin background which is partially transparent to IR, while the strokes that define both the lips and the eyes look minimal (Figure 8a–c).

3.1.3. Fourier Transform Infrared Spectroscopy in ATR Mode (FT-IR ATR)

FT-IR in ATR mode was performed on sample 2—which includes the stratigraphy from the original canvas to the varnish layer, and 3—which consists of the ground layer, the primer, the paint layers, and the varnish. The spectra collected on the varnish on both sample 2 and sample 3 show IR bands related to non-aged dry shellac resin (wax-free)—a standard material at the YOCOCU APS laboratory and in the material's spectrum in the database built by S. Vahur [25,26] (Figures 9 and 10). These similarities were confirmed by the literature, which identifies the characteristic peaks of shellac [31]. Specifically, the two peaks at 2858 and 2929 cm^{-1} correspond to the symmetric and asymmetric stretching vibrations of C-H, while the peak at 1710 cm^{-1} represents the C=O stretching vibration [32]. In addition, CH_2 bending molecular motions at 1462 cm^{-1} are present, while the bands at 945 and 928 cm^{-1} identify the C-H stretch of CH_2 of the alkene groups. The broad stretching band of the OH group is present in all the acquisitions—including the spectrum of the canvas (Figure 11)—with a maximum at 3351 cm^{-1}, which is characteristic for stretching vibration of the hydroxyl group in polysaccharides. The intensity increase in carbonyl group absorption peak at 1710 cm^{-1} with respect to the pure shellac is due to the esterification process, which occurs in the material with ageing, together with the overall modification of the fingerprint region of the C-O stretching vibrations at 1240, 1163, and 1039 cm^{-1} resulting from the ester, acid, and alcohol groups of the shellac [32–34]. However, differences between the standard material and the spectra collected are related to both the ageing of shellac and the heterogeneous nature of the varnish, which presents impurities from the underneath layers. For this reason, more specific and confident assumptions on the differences between the pure and the aged shellac are not possible within this framework. The spectrum collected on the back of sample 2 shows different peaks which can be related to both cellulose and glue-starch paste, which is often used in lining interventions (Figure 11) [35,36]. Common peaks are visible at 1158, 1334, 1367, and 1429 cm^{-1}, indicating C-O-H stretching vibrations of the alcoholic groups, O-H stretching vibration, and $-CH_2$ bending of pyranose ring [37,38]. However, characteristic bands of cellulose can be seen at 898, 1029, and 1110 cm^{-1}, showing definite peaks belonging to β-glycosidic linkage between glucose units, C-O-C pyranose ring vibration, and C-O stretching vibration, respectively [37,38]. Furthermore, the peak at 1633 cm^{-1} could identify the presence of absorbed water between the fibers, posing questions regarding the moisture content of the canvas [39].

The band related to the use of glue-starch paste can be clearly seen at 998 cm^{-1}, which represents the characteristic C-O stretching vibrations (Figure 11) [40]. Eventually, the analysis of the back side of sample 2 shows peaks at 1390 and 670 cm^{-1} related to C=O vibrations in the carbonate ion CO_3^{2-} [41], which can be attributed to the use of calcium carbonate or lead carbonate in the ground layer, as confirmed by SEM/EDS analyses (see Section 3.1.4).
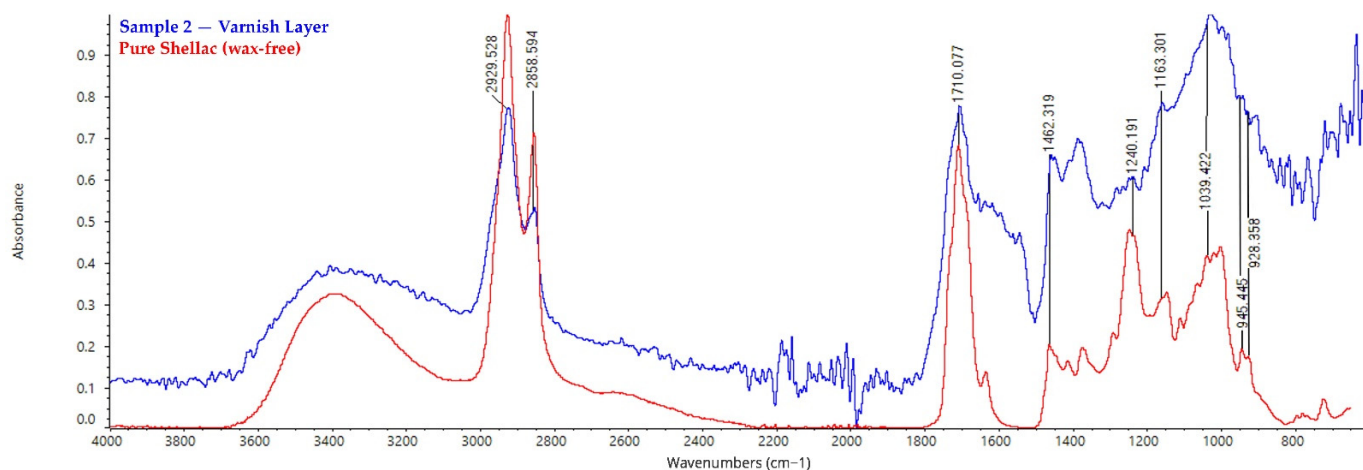
Figure 9. FT-IR ATR spectra collected on the front side of sample 2, which includes the original canvas, the ground layer, the primer, the paint layers, and the varnish: analysis of the varnish layer.
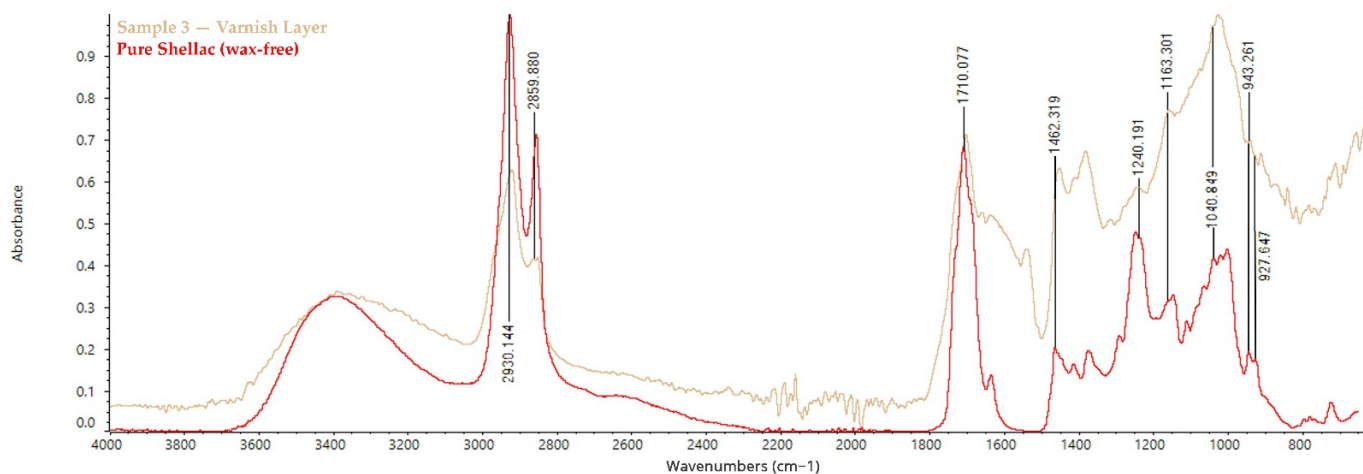
Figure 10. FT-IR ATR spectra collected on sample 3, which includes the ground layer, the primer, the paint layers, and the varnish: analysis of the varnish layer.
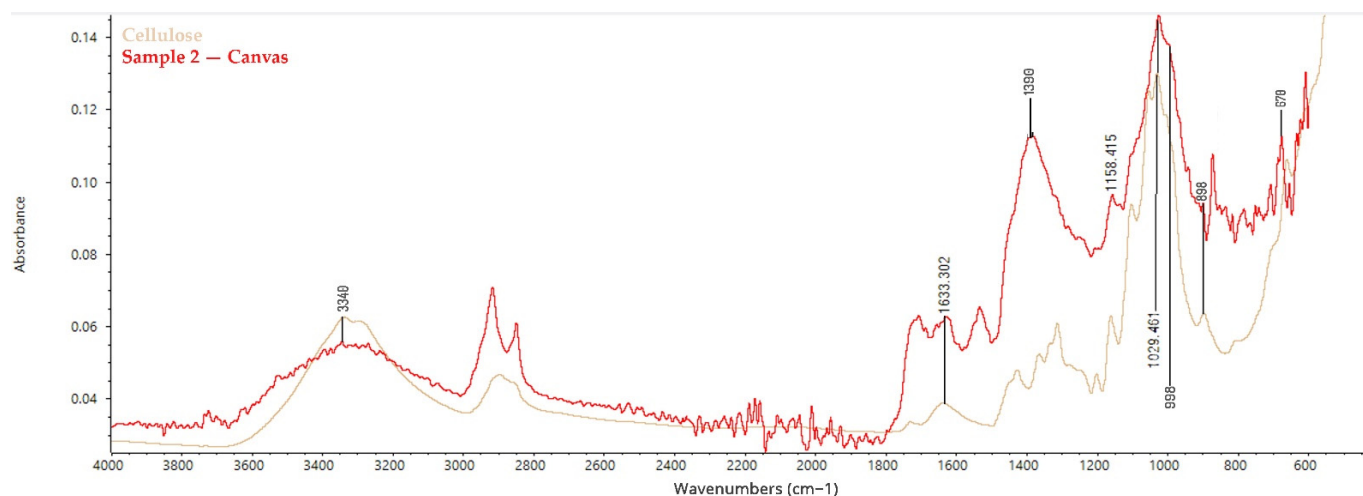

Figure 11. FT-IR ATR spectra collected on the back side of sample 2, which includes the original canvas, the ground layer, the primer, the paint layers, and the varnish: analysis of the canvas.

3.1.4. Scanning Electron Microscope Coupled with an Energy Dispersion Microanalytical System (SEM–EDS)

SEM/EDS analyses were performed on sample 1 and 2. Sample 1 was subjected to analysis using the back-scattered electron detector to make chemical elements with a higher atomic number appear with lighter grey contrast. When seen from the surface, sample 1 appears to be characterized by two external layers with low atomic contrast (spectra 1, 3, Figure 12a) applied on a layer consisting of elements with high atomic weight (spectra 2,4,5, Figure 12a), which appear to be on top of a low-contrast layer (spectrum 6, Figure 12a). In the external paint layers, the spectra collected showed the presence of elements such as iron (Fe), lead (Pb), calcium (Ca), and phosphorus (P) (Figure 12a, Table 3). These elements cannot be correlated with each other, suggesting that the blue area on the surface consists of an iron-based pigment, probably Prussian Blue, which is a ferric hexacyanoferrate. Iron only was detected since the cyan group is given by the union of a carbon atom and a nitrogen atom, which cannot be identified by SEM. The hypothesis is supported by other analyses carried out on Antonio Mancini's palette by 1928 and on a large number of paintings by the artist, which cover the years from 1868 to 1929 [2]. It was found that, among the blue colors, he clearly preferred Prussian Blue and Ultramarine Blue, sometimes also using Cerulean, while Cobalt Blue appears to be rarer.

Table 2. Elements detected through EDS analysis of the areas shown in Figure 12b.

Spectrum	C	O	Al	Si	P	S	Ca	Cr	Fe	Zn	Pb
Spectrum 1	47.1	32.5	1.3	2.3	2.4	1.8	4.6	1.2	3.7		1.2
Spectrum 2		29.2					7.3			1.5	63.5
Spectrum 3		47.4	3.5	3.2	7.4	2.6	14.9	1.1	6.5		13.5
Spectrum 4	47.4	34.5	1.2	2.9	1.7	1.1	7.00		5.1		
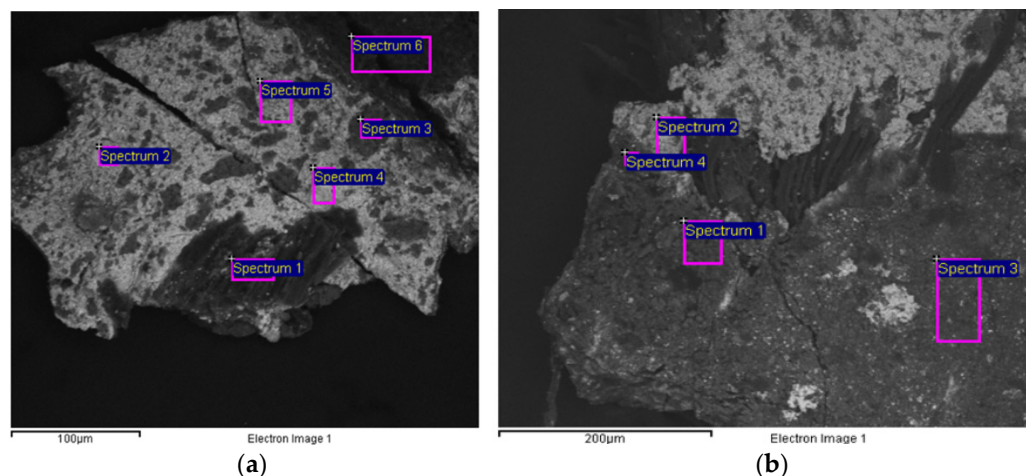
Figure 12. SEM images showing sample 1, which includes the ground layers and the paint layers. Indication of the areas on which the spectra were collected: analysis of a larger area of the sample (**a**) corresponding to the results in Table 3, and analysis of a detail of another portion of the sample (**b**) corresponding to the results in Table 2.

The presence of phosphorus on sample 1 is due to the use of Bone Black, calcium is related to both Bone Black and white pigments, while lead can be attributed to the presence of Lead White. This paint layer, consisting of Prussian Blue, calcium carbonate, Lead White, and Bone Black, is on top of a blue iron-based paint layer, probably Prussian Blue, which serves as a primer for the upper paint. The first ground layer shows the presence of zinc (Zn) and lead (Pb), which are related to the use of Zinc White and Lead White, respectively. As in other paintings between 1868 and 1911, this composition for the ground layer can be traced back to an industrial application [2].

Table 3. Elements detected through EDS analysis of the areas shown in Figure 12a.

Spectrum	C	O	Na	Al	Si	P	S	K	Ca	Fe	Zn	Pb
Spectrum 1	47.8	32.3				1.0	1.0		2.8	3.7		11.6
Spectrum 2		26.5	5.7						1.0			67.0
Spectrum 3	29.2	35.0							21.0	3.4		11.2
Spectrum 4		23.0							2.8			74.0
Spectrum 5	31.6	15.6							2.3			50.5
Spectrum 6		51.0	9.2	9.8	9.7	2.6	6.7	0.8	1.6		8.4	

Further investigation of the pictorial layers was performed on other sections of the sample (Figure 12b). The fragment confirms the stratigraphy and relative composition already detected in the first stage. However, the analysis of the pictorial layer shows the presence of chromium (Cr) as an additional chromophore element (spectra 1, 3, Figure 12b, Table 2), indicating the presence of Chromium Oxide Green, also detected in *L'enfant dans un grand fauteuil*, a painting of the same period (1875). Eventually, the presence of zinc together with lead confirms the use of both of them in the preparatory layer, showing similarities with the ground layer of *Acque basse* (1874).

As to sample 2, the backscattered electron image allowed definition of the presence of three layers, two of them showing dark grey contrast (spectra 1, 3, Figure 13a) and one of them a light contrast (spectrum 2, Figure 13a). The paint layers seem to be characterized by the same elements of sample 1, differing only in the purity of the layer adjacent to the preparation layer, which is characterized by the presence of iron, one more time suggesting the use of Prussian Blue (spectra 1, 3, Figure 13a, Table 5). The features of this layer are of particular interest: it seems that Antonio Mancini applied an oil primer presumably composed of Prussian Blue on top of the ground layer. This choice would have been extremely uncommon, since no primers were detected in other paintings of the artist whose stratigraphy is known [2]. Furthermore, the preparation layer consists of Lead White (spectrum 2, Figure 13a, Table 5), which can be linked to a ground layer applied by the artist, as in *Il padre dell'artista* (1890) [2]. Indeed, SEM/EDS analysis of the backside of sample 2, i.e., the ground layer, shows that it consists of two layers: one is adjacent to the canvas and is an industrial application of a mixture of Zinc White and Lead White (spectrum 1, Figure 13a, Table 5), while the upper one shows a high lead (Pb) content (Lead White) and was applied by the artist (spectra 2, 5, 6, Figure 13a, Table 5). The white ground layer appears to be a peculiar feature of Mancini's works: indeed, it was found in another five paintings by the artist belonging to the period between 1868 and 1911, namely, *Scugnizzo con l'ombrello* (1868), *Acque basse* (1874), *L'orfanello* (1886), *Il padre dell'artista* (1890), and *Fanciulla di profilo ridente* (1911) [2].

Table 4. Elements detected through EDS analysis of the areas shown in Figure 13b.

Spectrum	Al	Zn	As	Pb
Spectrum 1		23.3	54.7	22.0
Spectrum 2				100
Spectrum 3	20	80.0		-
Spectrum 4	3.2	96.8		-
Spectrum 5				100
Spectrum 6				100

The analysis of another portion of sample 2 confirms the results already reported. The chromophore elements of the paint layer's surface are iron, chromium, and phosphorus (spectra 1, 3, 4, 5, Figure 13b, Table 4), while the preparation layer adjacent to the paint layer consists of lead and calcium carbonate (spectrum 2, Figure 13b, Table 4), as in *L'orfanello*, made in 1886 [2].

(**a**)

(**b**)
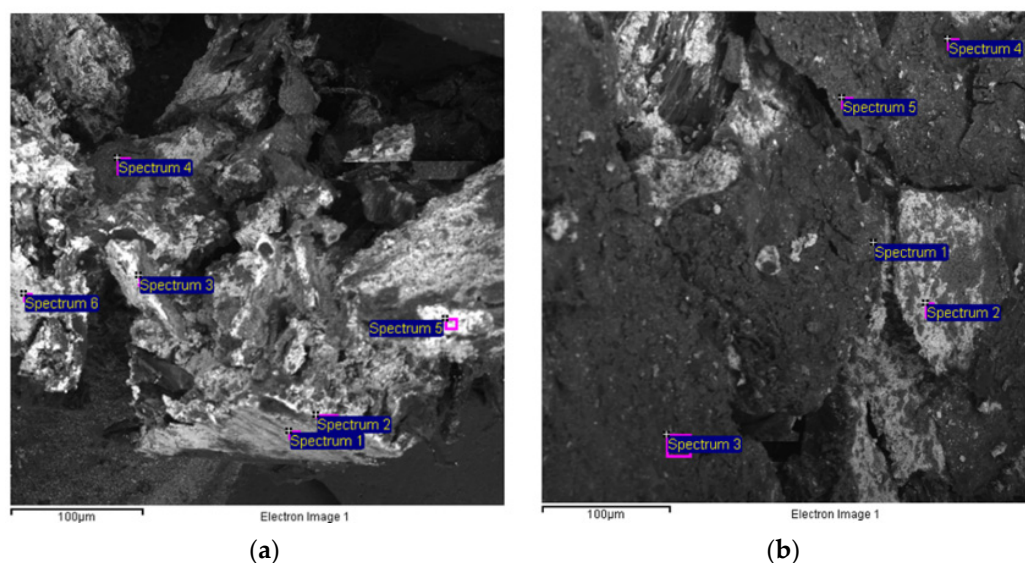
Figure 13. SEM images showing sample 2, which includes the whole stratigraphy, namely, the canvas, the ground layer, the paint layers, and the varnish. Indication of the areas on which the spectra were collected: analysis of a portion of the sample (**a**) corresponding to the results in Table 5, and analysis of another portion of the sample (**b**) corresponding to the results in Table 4.

Table 5. Elements detected through EDS analysis of the areas shown in Figure 13a.

Spectrum	C	O	Mg	Al	Si	P	S	Ca	Fe	Zn	Pb
Spectrum 1		67.0	1.3	3.7	4.6	5.7	3.0	10.1	2.9	1.8	
Spectrum 2		34.0						8.2			57.8
Spectrum 3	48.8	36.9		3.2	1.4		1.68	2.3	5.6		

3.2. Cleaning Tests

FTIR spectroscopy analysis in ATR mode allowed the identification of the finishing varnish as partially oxidized non-original shellac, which needed to be selectively removed due to its yellow/brownish tone which hides the original colors and definition of the figure.

The selected cleaning systems were applied to confined areas using a mask (Figure 14). Then, the cleaning performances were evaluated examining the surface, the cotton swabs, and the gels used for the treatment with the portable optical microscope DinoLite AM411-FVW at magnifications from $40\times$ to $220\times$, and at two illumination modes: visible light and UV light. The observation allowed the restorers to build a scoreboard for each cleaning system. According to the criteria used for the selection of the solvents, the restorers were asked to evaluate the following parameters: degree of solubilization, amount of removed varnish on the swab, respect of the criterium of minimum intervention, degree of selectivity during the removal of the varnish, and control of removal of the varnish.

Table 6 summarizes the restorer's evaluation of the cleaning effectiveness of the tested cleaning systems. The scale of evaluation varies within the following range: insufficient (+), poor (++), sufficient (+++), good (++++), excellent (+++++). The product that the restorer was most satisfied with was Polar Varnish Rescue GEL, an anionic surfactant mixed with acetals and gelled through hydroxypropylcellulose (5% *w/v*). The scale can be described as: Polar Varnish Rescue GEL > Green Varnish Rescue GEL > Green Varnish Rescue = Nanorestore Cleaning > Ethanol Anhydrous Absolute > Deionized water.
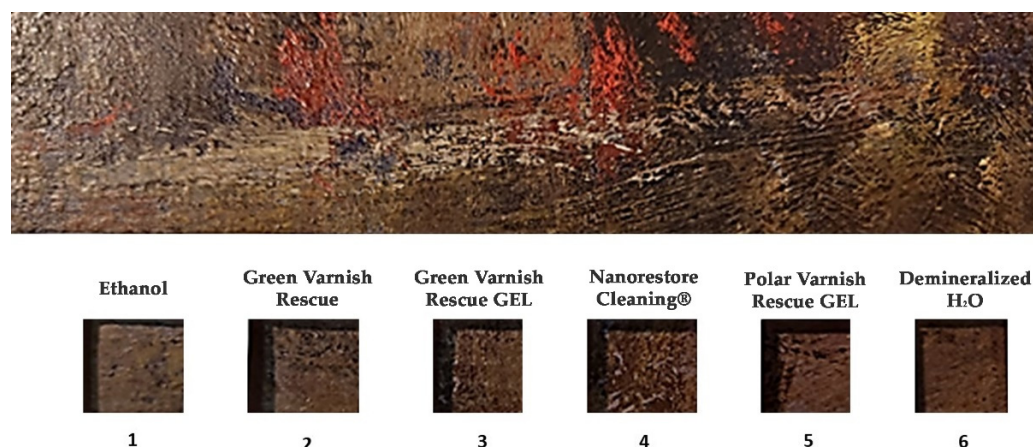
Figure 14. Areas treated during the cleaning tests. Squares dimensions: 1.5×1.5 cm.

Table 6. Restorer's evaluation of the tested cleaning systems.

Criteria	Ethanol	Green Varnish Rescue	Green Varnish Rescue GEL	Nanorestore Cleaning®	Polar Varnish Rescue GEL	Deionized Water
ID	1	2	3	4	5	6
Degree of solubilization	++	+++	++++	++	+++++	+
Removed varnish on the swab	+++	++++	++++	++	+++++	+
Minimum intervention	+++	+++	++++	++++	+++	+
Selective removal	++++	++++	+++++	++++	+++++	
Controlled removal	+++	++	+++	++++	+++++	+++++

The Green Varnish Rescue, using both the liquid and the gelled forms, was able to solubilize the varnish as well, respecting the criteria of minimum intervention (Table 7). In the other cases, the pictures collected show that the paint was not solubilized, although the surface increased its brightness (Table 7). However, this result was due to the removal of surface dirt and not to the solubilization of the shellac. Indeed, DinoLite images collected using UV light highlighted the persisting presence of the varnish on the areas treated with Ethanol (area n. 1), Nanorestore Cleaning® (area n. 4), and demineralized H_2O (area n. 6), still showing the yellow-green fluorescence identifying the shellac varnish. On the contrary, the areas cleaned using the Green Varnish Rescue—in the liquid form and as a gel, and the Polar Varnish Rescue GEL demonstrate the effective removal of the varnish layer, showing the blue fluorescence which characterizes the paint layer underneath. Thus, the images obtained using the DinoLite on the areas cleaned by the different products confirm that the Polar Varnish Rescue GEL proved to be the best-performing cleaning system for its respect of all the previously defined criteria.

Table 7. DinoLite images of the treated areas in VIS (1a, 2a, 3a, 4a, 5a, 6a, 1c, 2c, 3c, 4c, 5c, 6c) and UV light (1b, 2b, 3b, 4b, 5b, 6b, 1d, 2d, 3d, 4d, 5d, 6d) before (1a, 2a, 3a, 4a, 5a, 6a, 1b, 2b, 3b, 4b, 5b, 6b) and after (1c, 2c, 3c, 4c, 5c, 6c, 1d, 2d, 3d, 4d, 5d, 6d) the cleaning treatment: cleaning systems identified through the IDs in Table 6.
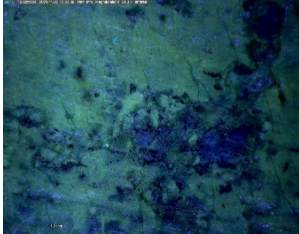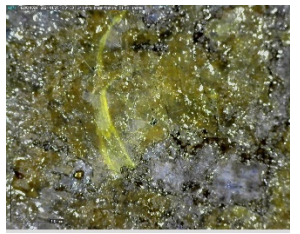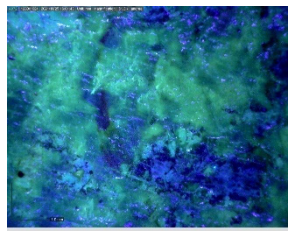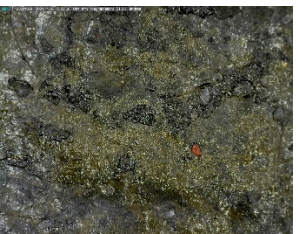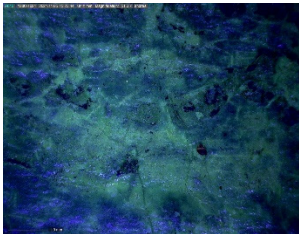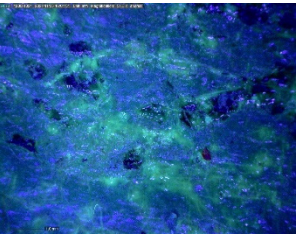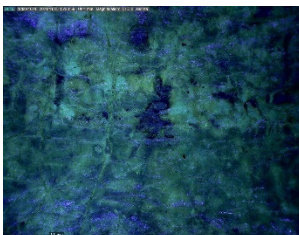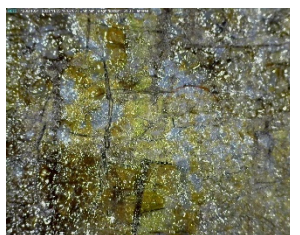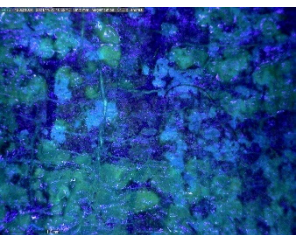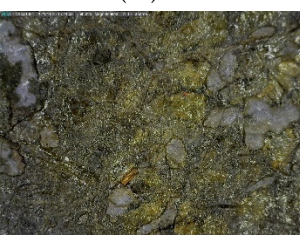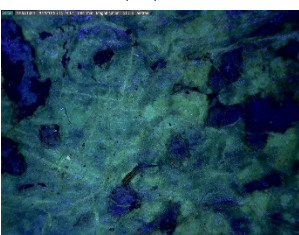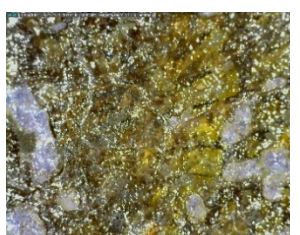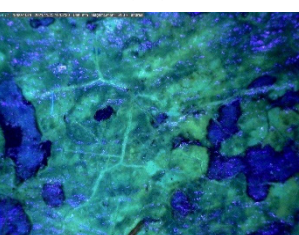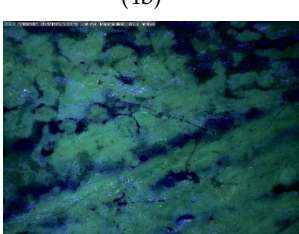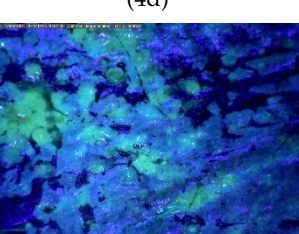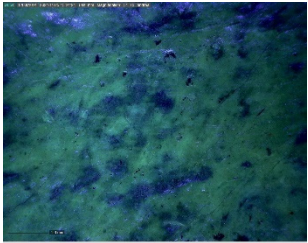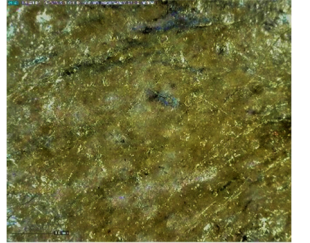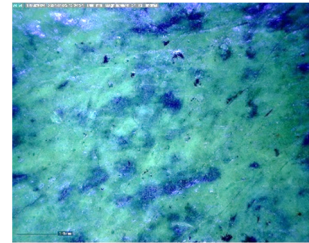
ID	Before Treatment		After Treatment	
	VIS	UV	VIS	UV
1	(1a)	(1b)	(1c)	(1d)
2	(2a)	(2b)	(2c)	(2d)
3	(3a)	(3b)	(3c)	(3d)
4	(4a)	(4b)	(4c)	(4d)
5	(5a)	(5b)	(5c)	(5d)

Table 7. *Cont.*

ID	Before Treatment		After Treatment	
	VIS	**UV**	**VIS**	**UV**
6				
	(6a)	(6b)	(6c)	(6d)

After the cleaning tests, the Polar Varnish Rescue GEL was tested on the same area of application of water, which was not effective, to optimize the number of steps or the contact time of the gel. It can be seen that the degree of solubilization is lower compared to the previous contact time (120 s), and was yet effective.

4. Discussion

As shown through the multi-analytical approach implemented, Mancini's palette did not change significantly from the 1870s, as mentioned in previous research [2]. Indeed, similarities were found comparing the constituent materials of *Il Venditore di Cerini* with the results obtained from the analysis of other paintings made by Mancini such as *Scugnizzo con l'ombrello* (1868), *Acque basse* (1874), *L'orfanello* (1886), *Il padre dell'artista* (1890), and *Fanciulla di profilo ridente* (1911). Even though the characterization of the original layers deepened the available information on Mancini's artistic technique, the main goals of the multi-analytical study were the identification and dating of the aged varnish. The characterization of the coating as a non-original aged shellac enabled the definition of the suitable Fd value to be used. The selection and implementation of potentially well-performing cleaning systems were selected among sustainable alternatives available in the market. Indeed, the present study aimed at promoting the use of new green materials for conservation purposes which can be easily and effectively used by restorers. The "greenness" of the products was regarded as an essential quality to be fulfilled, since hazardous substances are still widely used in the conservation field for cleaning treatments on artworks, even if they are recognized to be dangerous for both human health and the environment. Recently, greener methods have been explored through the implementation of bio-based, low-toxic solvents. YOCOCU APS is working in the same direction through the development of sustainable solutions capable of preserving the essential qualities of the artworks' materials while safeguarding both the operators' health and the environment. The materials tested in the present work represent the first promising results obtained from the research, which is currently proceeding in multiple directions.

The reason for the effective removal of the shellac varnish by both the Green Varnish Rescue and the Polar Varnish Rescue is twofold: the Fd value of the products, which is similar to the Fd known to be used for the removal of shellac, and the acetals' higher tendency to establish hydrogen bonds with the material to be removed. The high value of shellac's hydrogen bonding plays a significant role in the solvation mechanism. Indeed, the Polar Varnish Rescue has a greater tendency to establish hydrogen bonds, due to the constituent components, and the whole solubility is even further enhanced by the presence of an anionic surfactant.

Eventually, the use of other delivery systems could be considered in future experiments to evaluate the efficient dispersion and stability of both the Green Varnish Rescue and the Polar Varnish Rescue in gels other than cellulose ether-based gels.

5. Conclusions

The multi-analytical process implemented for the examination of *Il Venditore di Cerini* made by Antonio Mancini in 1878 enabled the characterization of the entire stratigraphy and the constituent materials of the oil painting on canvas. The analysis of the ground layers showed the presence of a first ready-prepared industrial ground layer, made of Zinc (Zn) White and Lead (Pb) White, which can be found in *Acque basse* (1874) as well. On top of it, a ground layer made of Lead White and, in some areas, also of calcium carbonate, was applied by Antonio Mancini himself, showing similarities with *Il padre dell'artista* (1890) and *L'orfanello* (1886). The oil primer—presumably composed of Prussian Blue, appears to be of particular interest, since it would have been detected on one of Mancini's works here for the first time.

The results obtained from the paint layers showed similarities between the pigments and the binder used by the artist in the present work and the ones present in other paintings by the Italian artist. The use of Prussian Blue appears to be a constant in Mancini's career, appearing both in his palette (1928) and *Scugnizzo con l'ombrello* (1868). Indeed, on top of the second ground layer, a blue oily primer made of Prussian Blue and a thin paint layer made of Prussian Blue and Chrome Green were identified by EDS. The tones of the paint appear to have been darkened through the use of Bone Black, identified by the presence of phosphorus and calcium with quantitative values sometimes referring to the stoichiometry of calcium phosphate. Multispectral imaging unearthed the restored areas and the original shapes of the figure, showing the absence of a graphic setting, while the fluorescence induced by UV radiation proved that the varnish is not original: it could not be traced back to execution stage, since it was applied on top of the signature of the artist.

The multi-analytical process succeeded in guiding the cleaning treatment on the painting though the characterization of both the original materials and the shellac varnish as a non-original layer which had to be selectively removed. The Polar Varnish Rescue GEL proved to be the best-performing green cleaning system, showing a good degree of solubilization while guaranteeing a selective removal of the aged varnish. The solvation mechanism relies on its Fd value, the presence of an anionic surfactant, and the ability of its constituents to establish hydrogen bonds with shellac. It can be easily applied, showing a good degree of solubilization and overall valuable qualities for cleaning treatments on works of art. Most importantly, it represents an alternative to more toxic solvents that are still widely used in the conservation field, since its components are known to be green chemicals capable of safeguarding both human health and the environment.

Institutional Review Board Statement: Not applicable.

Informed Consent Statement: Not applicable.

Data Availability Statement: Publicly available datasets were analyzed in this study to compare the acquired FT-IR spectra with already available spectra of standard materials. Data can be found here: http://cameo.mfa.org/wiki/Category:Materials_database (accessed on 22 March 2022), and here: https://spectra.chem.ut.ee/ (accessed on 21 March 2022).

References

1. Sues, G. Antonio Mancini and His Art. *Collect. Art Crit.* **1900**, *2*, 201. [CrossRef]
2. Frezzato, F.; Poldi, G.; Amadori, M.L. Antonio Mancini. Evoluzione tecnica di un realista visionario. In *Tecnica Della Pittura in Italia fra Ottocento e Novecento*; Sargon Editore: Venice, Italy, 2021.
3. Hiesinger, U.W. *Antonio Mancini: Nineteenth-Century Italian Master*; Philadelphia Museum of Art: Philadelphia, PA, USA, 2008.
4. Virno, C. L'evoluzione artistica: Tecnica, modelli, soggetti. In *Antonio Mancini. Catalogo Ragionato Dell'opera. I. La Pittura a olio. Su tela, Tavola, Carta e Specchio*; De Luca Editori d'Arte: Rome, Italy, 2019; pp. 1–31.
5. Macchia, A.; Aureli, H.; Colasanti, I.A.; Rivaroli, L.; Tarquini, O.; Sabatini, M.; Dattanasio, M.; Munoz, L.P.; Colapietro, M.; la Russa, M.F. In Situ Diagnostic Analysis of the Second Half of the XVIII Century "Morte di Sant'Orsola" Panel Painting Coming from Chiesa Dei Santi Leonardo e Erasmo Roccacorga (LT, Italy). *Int. J. Conserv. Sci.* **2021**, *12*, 1377–1390.
6. Crupi, V.; Fazio, B.; Fiocco, G.; Galli, G.; La Russa, M.F.; Licchelli, M.; Majolino, D.; Malagodi, M.; Ricca, M.; Ruffolo, S.A.; et al. Multi-analytical study of Roman frescoes from Villa dei Quintili (Rome, Italy). *J. Archaeol. Sci. Rep.* **2018**, *21*, 422–432. [CrossRef]
7. Anastas, P.T.; Warner, J.C. *Green Chemistry: Theory and Practice*; Oxford University Press: Oxford, UK, 1988.
8. Estévez, C. Sustainable Solutions—Green Solvents for Chemistry. In *Sustainable Solutions for Modern Economies*; RSC Publishing: London, UK, 2009; pp. 407–424. [CrossRef]
9. European Chemicals Agency (ECHA). Guidance on REACH. 2015. Available online: http://echa.europa.eu/guidance-documents/guidance-on-reach (accessed on 12 March 2022).
10. Macchia, A.; Sacco, F.; Morello, S.; Prestileo, F.; la Russa, F.M.; Ruffolo, S.; Luvidi, L.; Settimo, G.; Rivaroli, L.; Tabasso, M.L. Campanella. Chemical exposure in Cultural Heritage restoration: Questionnaire to define the state of the art. In *Scienza e Beni Culturali XXX*; Arcadia Ricerche: Bressanone, Italy, 2014.
11. CAMEO Materials Database. 2020. Available online: http://cameo.mfa.org/wiki/Category:Materials_database (accessed on 22 March 2022).
12. Teas, J.P. Graphic analysis of resin solubilities. *J. Paint. Technol.* **1968**, *40*, 19–25.
13. Hansen, C.M. *The Three Dimensional Solubility Parameter and Solvent Diffusion Coefficient: Their Importance in Surface Coating Formulation*; Danish Technical Press: Copenhagen, Denmark, 1967.
14. Carretti, E.; Natali, I.; Matarrese, C.; Bracco, P.; Weiss, R.G.; Baglioni, P.; Salvini, A.; Dei, L. A new family of high viscosity polymeric dispersion for cleaning easel paintings. *J. Cult. Herit.* **2010**, *11*, 373–380. [CrossRef]
15. Lazidou, D.; Teknetzi, I.; Karapanagiotis, I.; Ritzoulis, C.; Panayiotou, C. Poly(vinyl alcohol)-borax films as cleaning agents for icons. *Archaeol. Anthropol. Sci.* **2019**, *11*, 6259–6271. [CrossRef]
16. Baglioni, M.; Poggi, G.; Chelazzi, D.; Baglioni, P. Advanced Materials in Cultural Heritage Conservation. *Molecules* **2021**, *26*, 3967. [CrossRef]
17. Mastrangelo, R.; Chelazzi, D.; Poggi, G.; Fratini, E.; Buemi, L.P.; Petruzzellis, M.L.; Baglioni, P. Twin-chain polymer hydrogels based on poly(vinyl alcohol) as new advanced tool for the cleaning of modern and contemporary art. *Proc. Natl. Acad. Sci. USA* **2020**, *117*, 7011–7020. [CrossRef]
18. Pensabene Buemi, L.; Petruzzellis, M.L.; Chelazzi, D.; Baglioni, M.; Mastrangelo, R.; Giorgi, R.; Baglioni, P. Twin-chain polymer networks loaded with nanostructured fluids for the selective removal of a non-original varnish from Picasso's "L'Atelier" at the Peggy Guggenheim Collection, Venice. *Herit. Sci.* **2020**, *8*, 77. [CrossRef]
19. Baglioni, P.; Bonelli, N.; Chelazzi, D.; Chevalier, A.; Dei, L.; Domingues, J.; Fratini, E.; Giorgi, R.; Martin, M. Organogel formulations for the cleaning of easel paintings. *Appl. Phys. A* **2015**, *121*, 857–868. [CrossRef]
20. Striova, J.; Fontana, R.; Barbetti, I.; Pezzati, L.; Fedele, A.; Riminesi, C. Multisensorial Assessment of Laser Effects on Shellac Applied on Wall Paintings. *Sensors* **2021**, *21*, 3354. [CrossRef] [PubMed]
21. Green Conservation of Cultural Heritage, 4nd International Conference. 2022. Available online: https://www.greenconservationconference.com/ (accessed on 18 March 2022).
22. YOCOCU. Green Varnish Rescue. 2018. Available online: https://www.yococu.com/prodotti/green-rescue/?lang=it (accessed on 18 March 2022).
23. YOCOCU. Polar Varnish Rescue Safety Data Sheets. 2021. Available online: https://www.yococu.com/polar-varnish-rescue/?lang=it (accessed on 18 March 2022).
24. Moity, L.; Benazzouz, A.; Molinier, V.; Nardello-Rataj, V.; Elmkaddem, M.K.; de Caro, P.; Thiébaud-Roux, S.; Gerbaud, V.; Marion, P.; Aubry, J. Glycerol acetals and ketals as bio-based solvents: Positioning in Hansen and COSMO-RS spaces, volatility and stability towards hydrolysis and autoxidation. *Green Chem.* **2015**, *17*, 1779–1792. [CrossRef]
25. Database of ATR-FT-IR Spectra of Various Materials. 2019. Available online: https://spectra.chem.ut.ee/ (accessed on 21 March 2022).
26. Vahur, S.; Teearu, A.; Peets, P.; Joosu, L.; Leito, I. ATR-FT-IR spectral collection of conservation materials in the extende region of 4000–80 cm^{-1}. *Anal. Bioanal. Chem.* **2016**, *408*, 3373–3379. [CrossRef] [PubMed]
27. Cremonesi, P. *L'uso dei Solventi Organici nella Pulitura di Opere Policrome*; Il Prato: Saonara, Italy, 2004.
28. Burke, J. Solubility Parameters: Theory and Application. *Book Pap. Group Annu.* **1984**, *3*, 13–58.
29. Feller, R.L.; Bailie, C.W. Solubility of aged coatings based on dammar, mastic and resin AW-2. *Int. Inst. Conserv. Hist. Artist. Work* **1972**, *12*, 72–81. [CrossRef]

30. Center for Colloid and Surface Science (CSGI). Nanorestore Cleaning®. 2015. Available online: http://www.csgi.unifi.it/products/cleaning_ita.html (accessed on 17 March 2022).

31. Derrick, M.; Stulik, D.; Landry, J.M. *Infrared Spectroscopy in Conservation Science. Scientific Tools for Conservation*; J. Paul Getty Trust: Los Angeles, CA, USA, 1999.

32. Coates, J. Interpretation of Infrared Spectra, A Practical Approach. In *Encyclopedia of Analytical Chemistry*; Wiley: Chichester, UK, 2000; pp. 10815–10837. [CrossRef]

33. Striova, J.; Salvadori, B.; Fontana, R.; Sansonetti, A.; Barucci, M.; Pampaloni, E.; Marconi, E.; Pezzati, L.; Colombini, M.P. Optical and spectroscopic tools for evaluation Er: YAG laser removal of shellac varnish. *Stud. Conserv.* **2015**, *60*, S91–S96. [CrossRef]

34. Copestake, S. The ageing & stabilization of shellac varnish resin—An undergraduate research project at Imperial College. *Conserv. J.* **1994**, *11*, 13–14.

35. Abdullah, A.H.D.; Chalimah, S.; Primadona, I.; Hanantyo, M.H.G. Physical and chemical properties of corn, cassava, and potato starch. In *IOP Conference Series: Earth and Environmental Science, Proceedings of the 2nd International Symposium on Green Technology for Value Chains 2017 (GreenVC 2017), Jakarta, Indonesia, 23–24 October 2017*; IOP Publishing: Bristol, UK, 2018; Volume 160. [CrossRef]

36. Poulis, J.A.; Seymour, K.; Mosleh, Y. The creep performance of bio-based and synthetic lining adhesives at different environmental conditions. *Int. J. Adhes. Adhes.* **2022**, *114*, 103119. [CrossRef]

37. Hospodarova, V.; Singovska, E.; Stevulova, N. Characterization of Cellulosic Fibers by FTIR Spectroscopy for Their Further Implementation to Building Materials. *Am. J. Anal. Chem.* **2018**, *9*, 303–310. [CrossRef]

38. El-Sakhawy, M.; Kamel, S.; Salama, A.; Tohamy, H.S. Preparation and infrared study of cellulose based amphiphilic materials. *Cellul. Chem. Technol.* **2018**, *52*, 193–200.

39. Garside, P.; Wyeth, P. Identification of Cellulose Fibers by FTIR Spectroscopy: Thread and Single Fibre Analysis by Attenuated Total Reflectance. *Stud. Conserv.* **2003**, *48*, 269–275. [CrossRef]

40. Librando, V.; Minniti, Z. Ancinent and modern paper characterization by FTIR and Micro-Raman spectroscopy. *Conserv. Sci. Cult. Herit.* **2011**, *11*, 249–268. [CrossRef]

41. Kloprogge, J.T.; Wharton, D.; Hickey, L.; Frost, R.L. Infrared and Raman study of interlayer anions CO_3^{2-}, NO_3^{-}, SO_4^{2-} and ClO_4^{-} in Mg/Al-hydrotalcite. *Am. Mineral.* **2002**, *87*, 623–629. [CrossRef]